Device

Article

Isostatic pressing of multilayer pouch cells and its implications for battery manufacturing

Graphical abstract

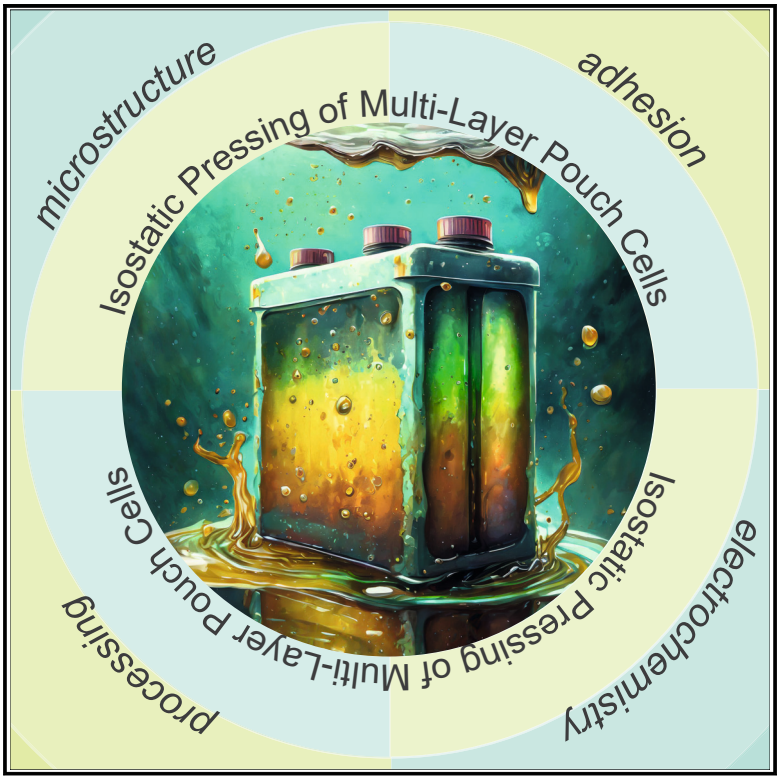

Highlights

- ISP processing results in uniform pressure for multilayer stacks
- ISP processing enhances cathode porosity, adhesion, and rate performance
- ISP's relevance extends to conventional and solid-state battery systems
- Integration of ISP into manufacturing promises efficiency and scalability gains

Authors

Marm Dixit, Chad Beamer, Rachid Essehli, ..., Timo Rabe, Mahalingam Balasubramanian, Ilias Belharouak

Correspondence

dixitmb@ornl.gov

In brief

This work shows how isostatic pressure (ISP) processing scales in multilayer cell stacks with focus on pressure distribution, microstructure evolution, and mechanical and electrochemical properties. Over a range of ISP conditions, we observe consistent and improved performance against baseline materials with ISP processing. With insights for solid-state battery development and seamless integration into production lines, ISP offers promising avenues for advancing battery technology.

2 Explore
Early prototypes with exciting performance and new methodology

Dixit et al., 2024, Device 2, 100370
August 16, 2024
https://doi.org/10.1016/j.device.2024.100370

CellPress

Please cite this article in press as: Dixit et al., Isostatic pressing of multilayer pouch cells and its implications for battery manufacturing, Device (2024), https://doi.org/10.1016/j.device.2024.100370

Device

CellPress

Article

Isostatic pressing of multilayer pouch cells and its implications for battery manufacturing

Marm Dixit,[1,3,*] Chad Beamer,[2] Rachid Essehli,[1] Anuj Bisht,[1] Ruhul Amin,[1] Mengya Li,[1] Jaswinder Sharma,[1] Timo Rabe,[2] Mahalingam Balasubramanian,[1] and Ilias Belharouak[1]

[1]Electrification and Energy Infrastructures Division, Oak Ridge National Laboratory, Oak Ridge, TN 37831, USA

[2]Quintus Technologies, Lewis Center, OH 43035, USA

[3]Lead contact

*Correspondence: dixitmb@ornl.gov

https://doi.org/10.1016/j.device.2024.100370

THE BIGGER PICTURE In this work, we investigate the impact of isostatic pressure (ISP) processing on multilayer pouch cells with an aim to elucidate its implications for battery manufacturing. Through ISP treatment of electrodes across various conditions, we unveil enhancements in porosity, adhesion, and rate performance compared to traditional manufacturing methods. By addressing challenges in electrode calendaring and particle cracking, ISP emerges as a pivotal facilitator for the realization of next-generation batteries, including solid-state variants. Integrating ISP into battery manufacturing processes promises to overhaul production throughput, particularly in formation and aging stages, where ISP seamlessly complements existing procedures. ISP's scalability for large-form-factor cells underscores its potential to propel advancements in energy storage on an industrial scale.

SUMMARY

We report a comprehensive investigation into the impact of isostatic pressure (ISP) processing on multilayer pouch cells. The study compares baseline electrodes fabricated using conventional manufacturing processes with isostatically pressed counterparts under varying conditions. Extensive characterization is carried out to assess the differences between baseline cells and those that underwent the isostatic pressing process. The electrochemical performance of the isostatically pressed cathodes was evaluated through impedance spectroscopy and galvanostatic charge-discharge tests. The results indicated that ISP led to notable improvements in porosity, adhesion, and rate performance compared to the baseline cathodes. This work elucidates the microstructural changes induced by ISP in lithium-ion battery cathodes and highlights the technology's promise for advancing battery manufacturing. The findings contribute to a better understanding of how ISP can be effectively integrated into cell assembly, fostering the development of more efficient and scalable battery manufacturing techniques for current Li-ion and solid-state batteries.

INTRODUCTION

Lithium (Li)-ion batteries have revolutionized the energy storage landscape, powering a wide range of applications, including portable electronics, electric vehicles, and grid-level energy storage.[1–4] The manufacturing process of these systems plays a crucial role in determining the performance, safety, and cost of Li-ion batteries.[5] Conventionally, Li-ion battery manufacturing involves several key steps, including electrode fabrication, electrolyte preparation, cell assembly, and formation/aging.[6] Electrode fabrication typically involves processes like slurry coating and calendaring, where active materials are mixed with binders and conductive additives to form electrode layers.[7] The calendaring process helps to achieve the desired electrode thickness, density, and porosity. After electrode fabrication, the cell assembly stage involves stacking the electrodes, separator, and filling electrolyte, followed by sealing the battery in a pouch can or cylindrical format. Finally, the formation/aging process involves subjecting the cells to controlled charging and discharging cycles to stabilize their initial performance.[8]

Solid-state battery (SSB) manufacturing, on the other hand, represents a new frontier in energy storage technology.[9] Unlike conventional Li-ion batteries, which use liquid electrolytes, solid-state batteries employ solid electrolytes, which offer advantages such as enhanced safety, higher energy density, and wider operating temperature ranges.[10] The manufacturing process for solid-state batteries differs from that of Li-ion batteries, with additional steps such as solid electrolyte synthesis, electrode-electrolyte integration, and solid-state interface optimization.[11–15] While both Li-ion and solid-state battery manufacturing

Please cite this article in press as: Dixit et al., Isostatic pressing of multilayer pouch cells and its implications for battery manufacturing, Device (2024), https://doi.org/10.1016/j.device.2024.100370

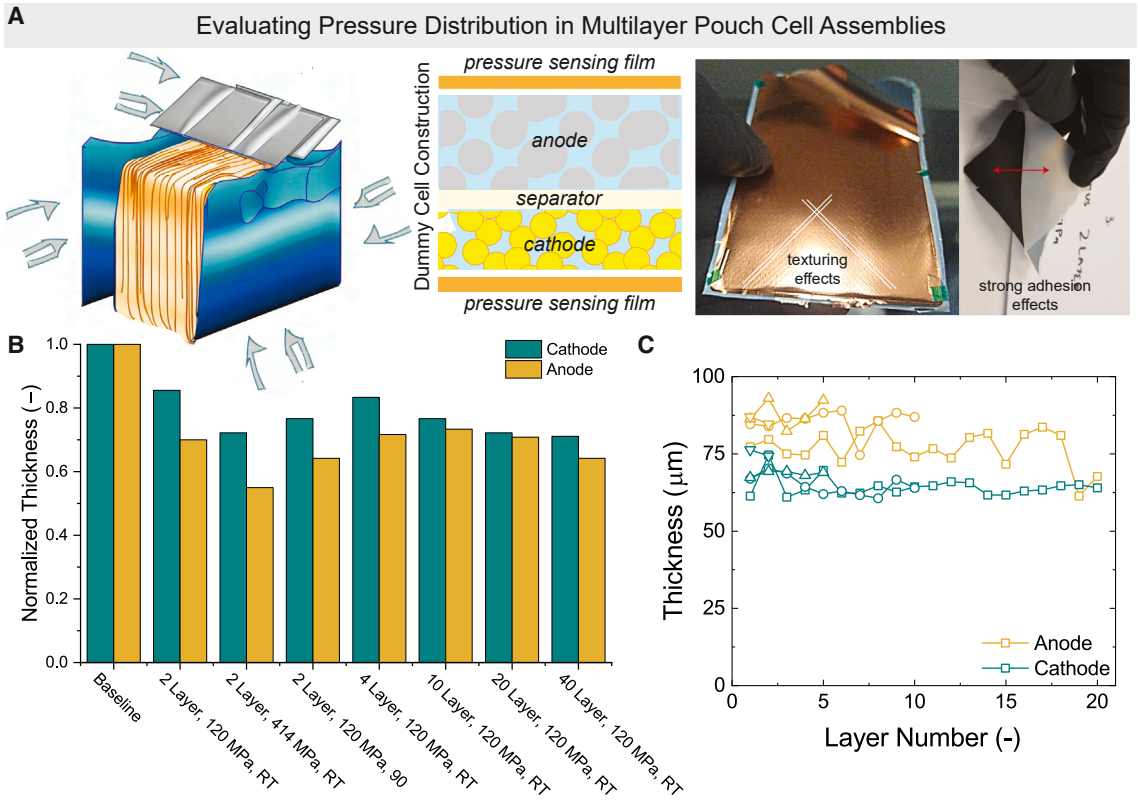

Figure 1. Isostatic pressing of multilayer pouch cells

(A) Schematic showing the motivation of our study: pouch cell isostatic pressing and the dummy cell generated for this study. Texturing of the current collector surface as well as the adhesion of the separator to the cathode are observed from disassembled dummy cells.

(B) Normalized changes in thickness compared to the baseline cathode and anode films with different isostatic pressing conditions and pouch cell configurations.

(C) The thickness of individual layers of cathode and anode films was observed in multilayer pouch cells. The symbols represent electrodes extracted from either 4-layer (▼), 10-layer (▲), 20-layer (●), or 40-layer (■) pouch cell stacks.

See also Figure S2.

processes share certain similarities, such as electrode fabrication and cell assembly, the integration of solid electrolytes in solid-state battery manufacturing introduces unique challenges.[16,17] These challenges include achieving efficient and uniform solid-state electrolyte deposition, optimizing the solid-state interfaces for low interfacial resistance, and ensuring compatibility between electrode materials and solid electrolytes.[18]

Isostatic pressure (ISP) is a scalable, manufacturing process that yields a high degree of control over local feature properties.[19] Isostatic pressing is a manufacturing process that involves applying uniform pressure to a material in all directions. There are different types of isostatic pressing, including hot isostatic pressing (HIP), warm isostatic pressing (WIP), and cold isostatic pressing (CIP). A recent perspective by our team showcased that this approach has been sporadically used for solid-state battery fabrication and integration, while it has hitherto not been leveraged in conventional Li-ion battery manufacturing.[19] ISP offers the potential to overcome the limitations of traditional manufacturing processes by providing precise control over critical parameters such as electrode density, thickness, and porosity. Specifically, for battery assembly and integration, CIP and WIP are two key available modes. WIP is a process similar to HIP but with lower temperature and pressure. WIP is typically performed at temperatures ranging up to 200°C, which allows for densification of materials without altering their microstructure. CIP involves applying pressure to a material at room temperature, which causes the material to deform plastically and become denser. The pressure in CIP is typically between 100 MPa and 700 MPa, which is higher than the pressure used in HIP and WIP. In recent literature, the role of and need for isostatic pressing for processing and integration of solid-state batteries is clearly highlighted.[9] ISP of cathode films has been shown to increase the volumetric energy density as well as cycling performance at high rates for lithium iron phosphate (LFP)-based materials.[20] Lee et al. demonstrated a solid-state pouch cell with an Ag-C interlayer processed with WIP that exhibited high energy density (>900 Wh kg^{-1}), stable Coulombic efficiencies (>99.8%), as well as long cycle life (1,000 cycles).[21] Fiedler et al. used a dry processing approach for composite cathode and separator fabrication along with ISP for integration in sulfur-based solid state pouch cells, yielding good cycling and rate performance.[22] For solid electrolytes themselves, isostatic pressing has been shown to improve density and transport properties, leading to improved electrochemical performance.[14,23–29]

Please cite this article in press as: Dixit et al., Isostatic pressing of multilayer pouch cells and its implications for battery manufacturing, Device (2024), https://doi.org/10.1016/j.device.2024.100370

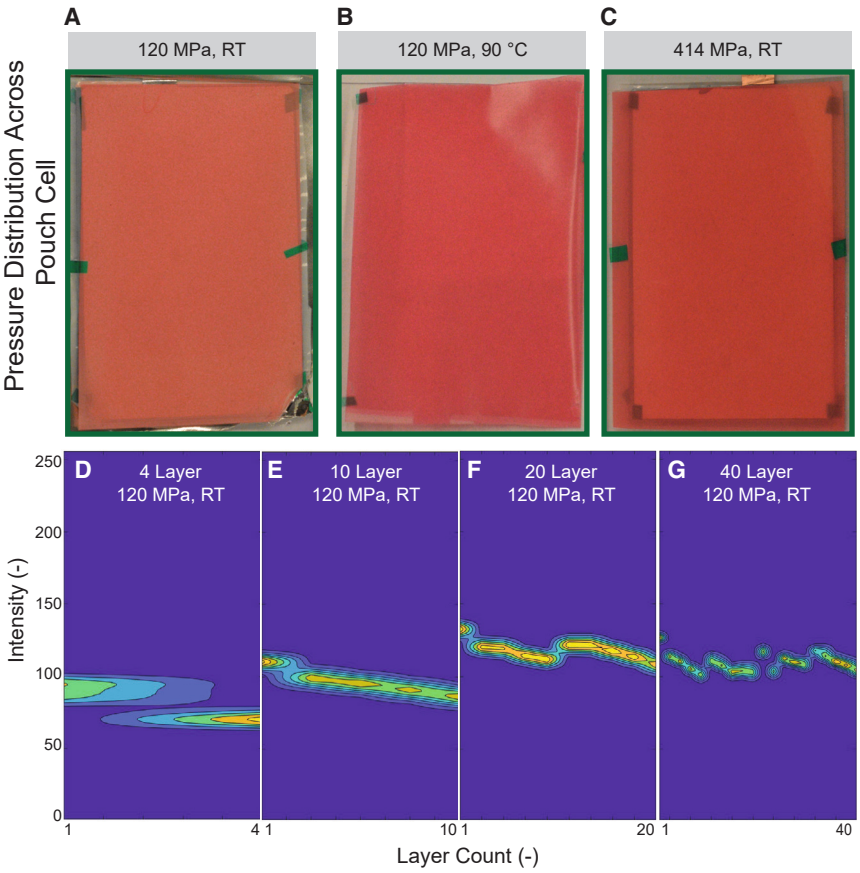

Figure 2. Analysis of pressure distribution

(A–C) Optical images of the pressure films placed inside the dummy pouch cells that underwent isostatic pressing under (A) 120 MPa, RT; (B) 120 MPa, 90°C; and (C) 414 MPa, RT conditions.

(D–G) Intensity profile calculated over the optical image for (D) 4-layer, (E) 10-layer, (F) 20-layer, and (G) 40-layer multilayer pouch cells. These cells were all isostatically pressed under 120 MPa, RT conditions.

See also Figures S3–S6.

Overall, ISP has seen a steady growth in being employed for solid-state battery manufacturing for proof-of-principle demonstrations with single-layer cells. However, the impact of ISP on multilayer pouch cells, which are commonly used in batteries, remains unexplored. Specifically, the questions of pressure distribution and structural and microstructural changes as well as the impact of ISP on electrochemical performance are not answered. This paper aims to address this research gap by evaluating the impact of ISP on multilayer pouch cells, focusing on conventional Li-ion battery technology. Specifically, we employ dummy pouch cells with conventional Li-ion battery materials to carry out this study. The investigation delves into several pressure-temperature dependencies to identify the optimized ISP conditions for achieving desired effects on pouch cells ranging from 2 layers to 40 layers. By assessing the performance, cycle life, and capacity of ISP-processed multilayer pouch cells, we aim to quantify the benefits and limitations of this technology in enhancing battery performance and reliability.

Furthermore, this study acknowledges the broader implications of ISP in the context of solid-state battery manufacturing. The insights gained from evaluating ISP in conventional Li-ion battery materials can potentially inform the development and optimization of solid-state battery fabrication processes. This highlights the dual significance of the research, as it contributes to the advancement of both conventional and solid-state battery technologies. This paper presents an in-depth investigation into the impact of ISP on multilayer pouch cells, shedding light on its potential to improve the performance and reliability of Li-ion batteries. The findings from this study will contribute to the ongoing efforts to optimize battery manufacturing processes, ultimately facilitating the widespread adoption of Li-ion batteries in various applications, including solid-state battery technologies.

RESULTS AND DISCUSSION

Isostatically pressed dummy pouch cells were extracted and examined in a dry room at the Department of Energy's Battery Manufacturing Facility at Oak Ridge National Laboratory (ORNL). It was observed that the vacuum seal of the pouch cell itself, along with the double-bagging approach used to isolate the pouch cell from the isostatic pressing fluid (oil), was extremely effective. All pouch cells were extracted from the plastic sealing bags without any contamination. On extracting the individual layers within the pouch cells, several notable differences were observed compared to the stacks found in conventional pouch cells. After isostatic pressing, the trilayer assembly of cathode-separator-anode had become rigid and could be handled as a single unit. In contrast, without the addition of electrolyte, electrostatic interaction between the separator and the electrodes makes this assembly typically difficult to handle. In addition, strong texturing of the current collector was observed with the isostatically pressed pouch cells (Figure 1A). This texturing is imprinted on the current collector from the plastic sealing bag used for encapsulating the pouch cells. Further, adhesion of the separator to the cathode was observed, where some mechanical effort was required to take the two layers apart (Figure 1A). Without isostatic pressing, there is typically no adhesion between these two layers, even after undergoing the vacuum sealing process.

One major impact of isostatic pressing is in the compaction and densification of materials. To assess the impact of the ISP process on film compaction, we assessed the thickness of the individual cathode and anode layers from all the pouch cells (Figure 1B). The individual layers of the single- and multilayer isostatically pressed pouch cells were extracted from the packaging.

Please cite this article in press as: Dixit et al., Isostatic pressing of multilayer pouch cells and its implications for battery manufacturing, Device (2024), https://doi.org/10.1016/j.device.2024.100370

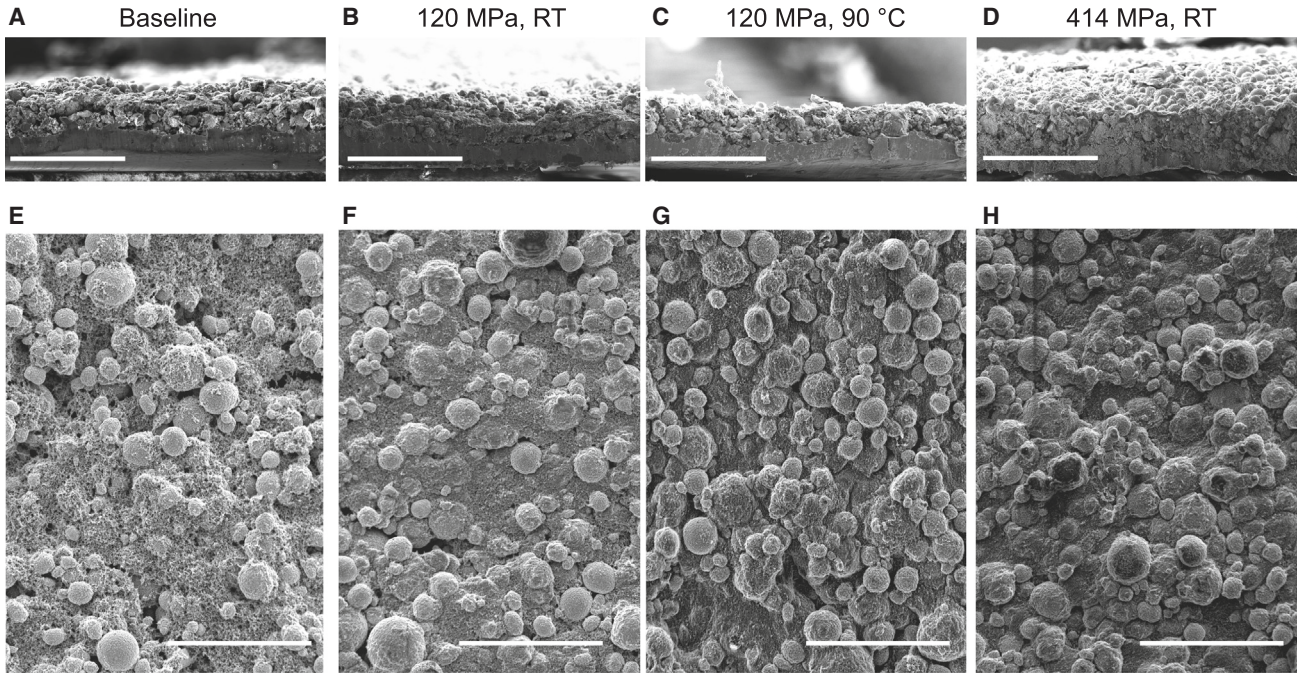

Figure 3. Morphology analysis of the cathode films

Shown are SEM images of cross-sectional and planar views of (A and E) baseline cathode material and the cathode films extracted from single-layer pouch cells isostatically pressed under (B and F) 120 MPa, RT; (C and G) 120 MPa, 90°C; and (D and H) 414 MPa, RT conditions. All scale bars represent 50 μm. See also Figure S7.

Subsequently, the individual layer thicknesses were measured using a micrometer. The raw thicknesses of the individual layers are reported in Figure S2. For single-layer cells, up to five measurements of the thickness of the cathode and anode were taken to estimate the average thickness of the film. For multilayer cells, the thickness was measured similarly across each of the layers, and the average was reported for the cell. We observe that ~20%–30% reduction in thickness is observed for the cathode films, while a 30%–50% reduction was observed for the anode films. We interpret this results in a 2-fold fashion. First reason for higher compaction could be arising from the higher initial porosity of the anode layers. Second, the materials of the anode (graphite, binder) have lower mechanical properties (*viz.* modulus, strength) that lead to higher densification at the pressures applied. The raw thickness values for all electrodes are reported in Figure S2. This essentially indicates a high level of calendaring of these electrode films with very low anticipated porosity (<15%). It should be noted that, even with this high degree of calendaring, the structural integrity of the current collector was not compromised. In conventional processing, very high calendaring pressures tend to rupture and destroy the current collector films. This is a key result indicating that ISP processing can aid significantly in streamlining the battery manufacturing process. For conventional Li-ion batteries, we anticipate that it can replace the calendaring step with the added advantages of improving electrolyte wetting and reducing the time for formation and aging cycle, which is a current bottleneck for Li-ion battery processing. For solid-state batteries, coupling the integration of cells and calendaring into a single step will offer several techno-economic benefits. The maximum compaction for the electrode films is observed for the single-layer pouch cells pressed at 414 MPa and room temperature. WIP at 90°C and 120 MPa for a single-layer pouch cell affords slightly higher compaction compared to the pouch cell pressed at room temperature at the same pressure. For multilayer pouch cells, it is seen that increasing the number of layers within the cell leads to a slightly better compaction of the layers. We anticipate that strong interactions between the layers and pouch cell material lead to this slight increase. Within multilayer cells, layer-to-layer variation is low and can be correlated back to variation in the feedstock electrodes used (Figure 1C).

Isostatic pressing is typically employed industrially with solid components, where the pressure distribution assessment is only carried out on the outer surface of the part. Due to the fundamentals of operation, the pressure on the outer surface of ISP parts is uniform. However, with battery cells, it is necessary to understand the distribution of pressures within the different layers of the cell itself. So far, no studies have investigated the internal pressure distribution in multilayered components exposed to ISP conditions. Employing a pressure-sensing film within the construction of the dummy cell, we enable a direct, *in-situ* measurement of pressure distribution as a function of the isostatic pressing conditions. For the single-layer pouch cells, the optical images for the pressure films from within the pouch cells are shown in Figures 2A–2C. These pressure films were originally white and, after pressure, turned pink. Differences in shades of color indicate variations in pressure within the films. For all single-layer films, no variations were detected

Please cite this article in press as: Dixit et al., Isostatic pressing of multilayer pouch cells and its implications for battery manufacturing, Device (2024), https://doi.org/10.1016/j.device.2024.100370

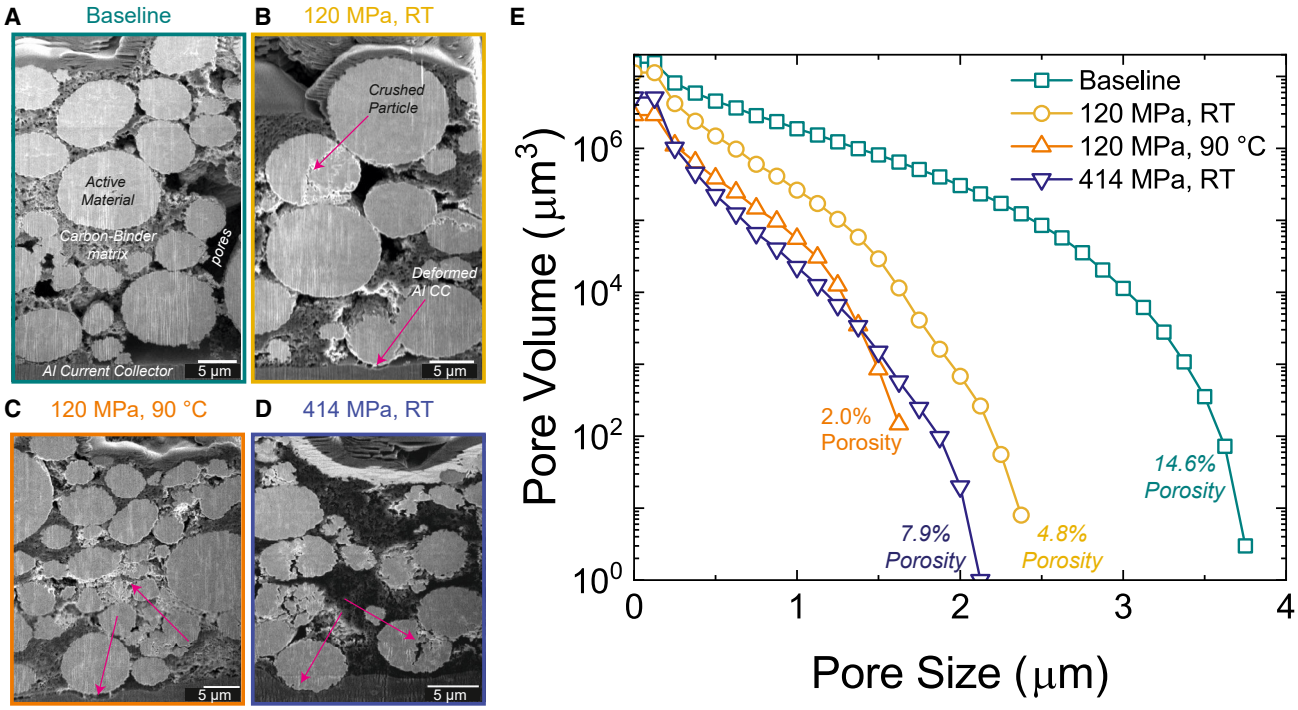

Figure 4. Cross-sectional microstructure and porosity analysis of cathodes

(A–D) FIB-SEM cross sections of the (A) baseline; (B) 120 MPa, RT; (C) 120 MPa, 90°C; and (D) 414 MPa, RT processed cathode films.

(E) Porosity and pore-size distributions of the baseline and ISP processed cathode films estimated from the FIB-SEM tomography datasets.

See also Figures S8–S12 and Videos S1–S4.

visually. To assess the multilayer films, we plotted the intensity profile (0–255) across the different layers of the cells (Figures 2D–2G). The raw images of the pressure films for all multilayer pouch cells are shown in Figures S3–S6. Across the layers, the intensity profiles remain consistent, with some notable exceptions. It is observed that the first layer always has a lighter shade, indicating a lower effective pressure on that film. The exact reason for this behavior is not understood yet, but we anticipate that this can be mitigated through the design of fixtures to hold the cells within the ISP system. Other than that, the pressure distribution is exceptionally uniform for all multilayer pouch cells. This is the first time that the pressure distribution for multilayer cells has been showcased, and the results show that the ISP can be effectively used to distribute pressure uniformly over large pouch cells.

The microstructure and morphology of the baseline cathode and isostatically pressed cathodes under three different conditions were examined using scanning electron microscopy (Figure 3). Cross-sectional and top-down scanning electron microscopy (SEM) images were acquired to gain insight into the electrode's structural characteristics. The baseline cathode, which underwent conventional coating and calendaring processes, exhibited a typical morphology, and the presence of pores was evident within the structure (Figures 3A and 3E). In contrast, the isostatically pressed cathodes under the three different conditions revealed a much denser microstructure consistent with the reduction in thickness for these conditions. The cross-sectional SEM images clearly show improved electrode density and enhanced interparticle contact within the active material. It is noteworthy that, even at very high ISPs, the cathode particles observed in the top-down images do not show any signs of microstructural deterioration/cracking. The presence of darker features on top of the cathode isostatically pressed at 414 MPa (Figure 3H) could likely correspond to a trace separator that might have adhered to these particles that underwent degradation under the electron beam. Similarly, the baseline and isostatically pressed anodes were examined by SEM (Figure S7). Isostatically pressed anodes show similar densification behavior as observed for the cathode films. Similar to the cathode films, no structural damage to the anode particles was observed on the surface of the anode films. To further assess the microstructural evolution, we carried out focused ion beam (FIB)-SEM tomography of the baseline and isostatically pressed electrodes.

FIB-SEM images of baseline and isostatically pressed cathodes are shown in Figures 4A–4D. The supplemental information also contains video files that show cross-sectional FIB-SEM tomography images for these systems. It is worth noticing that the area of interest covers the entire thickness of the cathode and consists of active material, carbon-binder matrix, pores, and the Al current collector. When the cathode was pressed isostatically under 120 MPa at room temperature, particle crushing along with some microcracks can be observed (pointed region in Figure 4B). Deformation of the current collector is also evident at the interface of the particle and the aluminum foil, which could

Please cite this article in press as: Dixit et al., Isostatic pressing of multilayer pouch cells and its implications for battery manufacturing, Device (2024), https://doi.org/10.1016/j.device.2024.100370

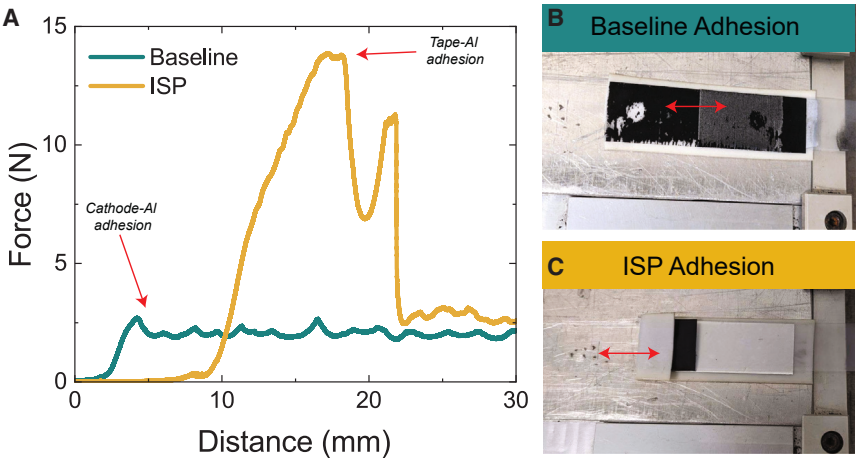

Figure 5. Adhesion measurements of cathode films

(A) Force-distance measurement from the adhesion test carried out for the basline and the ISP-processed material. The ISP condition for the cathode used for this test was 120 MPa, RT. Note that the highest force achieved by the ISP material does not indicate the adhesion of the coating but the tape to the Al backing plate.

(B and C) Optical image of the (B) baseline and (C) ISP-processed cathode after the peel testing. See also Videos S5 and S6.

be due to the isostatic pressing. By increasing the temperature to 90°C while maintaining the same pressure (120 MPa; Figure 4C), similar phenomena, such as crushed particles and a deformed current collector, can be seen.

However, when the isostatic pressing pressure was increased to 414 MPa at room temperature, significantly increased particle-current collector contact became visible with no gaps in between (Figure 4D). It is likely due to some welding effect because of the higher pressing pressure, which can also explain the ultra-strong adhesion that was observed in a peeling test (Figure 5). Pore size and pore volume information was obtained from subsequent image processing (Figure 4E). Notably, isostatic pressing leads to decreased pore size and porosity values within the cathode in comparison with the baseline sample, even though microcracks are presented and being considered as pores. Meanwhile, applying high temperature during isostatic pressing can further decrease the porosity but cannot trigger welding effects until a certain high pressing pressure is realized (414 MPa). Particle cracking observed with high ISPs can potentially be a challenge for long-term stability. Optimizing the time-temperature-pressure conditions for isostatic pressing should provide an avenue to mitigate the severity of the particle cracking observed. However, control experiments to achieve an equivalent degree of compaction through a traditional calendaring process with identical baseline electrodes yields significant damage to the integrity of the punched cathode films (Figure S8). We employed single- and multipass approaches to achieve identical levels of compaction achieved from ISP processes, and it was clearly observed that the cathode films cannot sustain this processing approach. Both surface as well as cross-sectional images from these calendered electrodes show significant damage to the cathode particle structure (Figures S9 and S10). The current collectors on these calendered electrodes also show significant damage through rupture and cracking (Figure S11). In contrast, the ISP-processed electrodes, for single-layer as well as multilayer pouches, resulted in excellent condition of the electrode films (Figures 1A, inset, and S12) with no damage to the integrity of the films. This presents a unique advantage of the isostatic pressing approach to achieve a high degree of compaction of electrode films compared to conventional calendering approaches.

The adhesion strength measurement studies revealed that ISP-processed cathodes have at least an order of magnitude higher adhesion strength with current collectors when compared to the adhesion strength of conventionally processed cathodes (Figure 5). The adhesion strengths were measured by using a peel tester (explained under experimental procedures; see supplemental information for a video of the peel test). During adhesion strength measurements, it was observed that the ISP-processed cathode layer was so strongly adhered to the current collector that, instead of peeling the cathode layer, the double-sided tape was peeled off the steel plate (Figure 5C). Therefore, in reality, we could only measure the adhesion strength of double-sided tape with the steel plate, and the adhesion strength of the ISP-processed cathode was beyond the strength of the double-sided tape adhesion strength with the steel plate. However, in the case of a conventionally processed cathode, a clean peeling of the cathode layer from the current collector was observed (Figure 5B). We could not measure the exact adhesion strength of ISP-processed cathodes to the current collector due to experimental limitations. However, it can be confidently stated that ISP-processed cathodes have at least an order of magnitude higher adhesion strength with the current collector than those of the conventionally processed electrodes. The higher adhesion strength is highly sought after because it lowers the chances of the cathode peeling off from the current collector during long-term cycling.

The preservation of the crystal structure of the cathode and anode during processing is of paramount importance in ensuring the integrity and performance of the energy storage system. The crystal structure, particularly of the $LiNiMnCoO_2$ (NMC) cathode, plays a pivotal role in dictating the electrochemical properties and overall efficiency of the battery. Any deviation from the ideal crystal arrangement can have profound implications on the cell's capacity, cycling stability, and rate capability. Therefore, maintaining the crystal structure during processing, such as isostatic pressing, is critical for the successful performance of pouch cell batteries. In our study, we investigated the impact of isostatic pressing on the crystal structure of NMC cathodes within both single-layer and multilayer pouch cells (Figures 6 and S13). Our X-ray diffraction (XRD) results reveal that, across the range of pressures tested, the crystal structure of the NMC cathode remains remarkably stable. This is true even for the cell processed at higher temperature of 90°C (Figure S13). This observation is

Please cite this article in press as: Dixit et al., Isostatic pressing of multilayer pouch cells and its implications for battery manufacturing, Device (2024), https://doi.org/10.1016/j.device.2024.100370

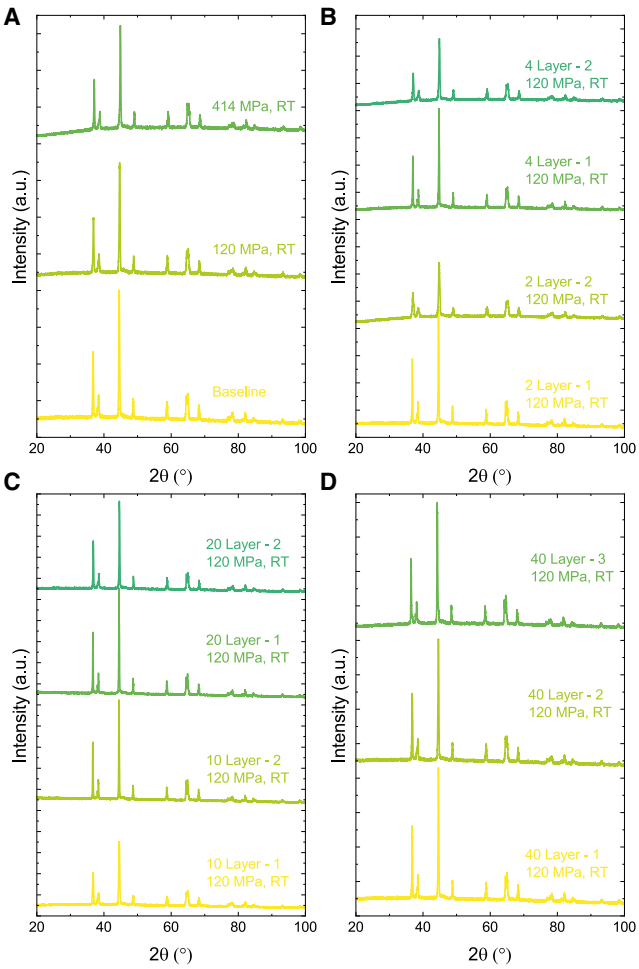

Figure 6. Structural analysis of cathode films

(A) XRD patterns of the baseline cathode and cathode processed in a single-layer pouch cell under 120 MPa, RT and 414 MPa, RT conditions.

(B–D) XRD patterns from cathode films extracted from (B) 2-layer and 4-layer, (C) 10-layer and 20-layer, and (D) 40-layer pouch cells. These pouch cells were isostatically pressed under 120 MPa, RT conditions. From multilayer cells, the cathode films were extracted to represent the complete film stack.

significant, as it suggests that the applied pressures do not induce structural changes in the cathode material, thereby preserving its electrochemical functionality. However, our analysis also unveiled changes in the intensity of XRD peaks, implying potential alterations in the orientation of crystal domains within the cathode (Figure 6D). The variation in intensity could signify a preferential orientation of crystal planes under the influence of isostatic pressing. Understanding the mechanism behind such preferential orientation is crucial, as it can influence the overall electrochemical performance of the pouch cell. Indeed, recent work on understanding cathode electrolyte interface (CEI) for single-crystal cathode particles in SSBs showed that certain facets of the cathode show much higher cycling stability, highlighting the need for preferential orientation.[30] Further, even with metal anode systems, orientation of the Li metal has been shown to greatly impact the reversibility of the plating and stripping.[31] These findings open the door to further investigations aimed at elucidating the orientation mechanisms in detail. To comprehensively assess the impact of isostatic pressing on the orientation of crystal domains within the NMC cathode, future research endeavors should delve into more detailed analyses, such as electron microscopy and additional crystallographic techniques. This will enable a thorough understanding of the interplay between applied pressures and crystallographic orientation, facilitating the optimization of manufacturing processes for enhanced pouch cell performance.

Impedance spectroscopy for the coin cells assembled from the baseline electrodes as well as the isostatically pressed samples are shown in Figure 7. The as-assembled cells all show similar profiles, with a semi-circular feature followed by a diffusion tail. The isostatically pressed samples showed a slightly lower total cell resistance compared to the baseline electrode. Similarly, after the formation cycle, the isostatically pressed films show much lower interfacial resistance. A detailed analysis of the impedance spectra and fitting is shown in Figures S14 and S15, and the equivalent circuit used is described in the supplemental information. The obtained individual resistance components are compared in Table 1 for each cell for the four different processing conditions. At least two cells were evaluated for the electrode of each processing condition. It is discernible from Table 1 that the magnitude of ohmic and interfacial cell resistance is quite low both before and after formation cycles. It should be noted that the ohmic and interfacial resistance of baseline cells are much higher compared to the isostatic processing electrodes after the formation cycle. Note that the R2 value is gradually decreased from baseline to 414 MPa room temperature (RT) samples (Table 1). The R3 value is reduced significantly compared to the baseline cell; however, the obtained data are not changed chronologically. This might be due to the insignificantly low value, which is within the error margin of the fitting parameters. The lower interfacial resistance with isostatically pressed electrodes could arise from several reasons: a large electrode surface area due to cracking, potentially homogeneous contact with the SEI film compared to baseline electrodes, or even due to improved wetting with the liquid electrolyte. Further work needs to be carried out to assess the origin of the improved interfacial resistance.

The formation cycles for all of the systems show similar behavior and Coulombic efficiencies in the initial cycles (Figure S16). The full cells were cycled under nominal C/3-C/3 conditions at 30°C. Overall, the isostatically pressed samples performed on par with the baseline materials (Figure 8). After 100 cycles, the baseline materials showed a retention of 83%. The cells formed from the dummy cells isostatically pressed at 120 MPa, RT condition; 120 MPa, 90°C; and 414 MPa, RT conditions similarly show retention of 80%, 85%, and 85%, respectively. The polarization curves from these cells (Figure S17) show typical profiles as expected from NMC-graphite systems. For the cells made from multilayered dummy cells, the results are similar in terms of capacity retention across all cells tested (Figure 9). On average, the cells from the four-layer dummy cell showed around ~87% retention, 10-layer cells showed around 85%, 20-layer cells showed around 81%, and 40-layer cells

Please cite this article in press as: Dixit et al., Isostatic pressing of multilayer pouch cells and its implications for battery manufacturing, Device (2024), https://doi.org/10.1016/j.device.2024.100370

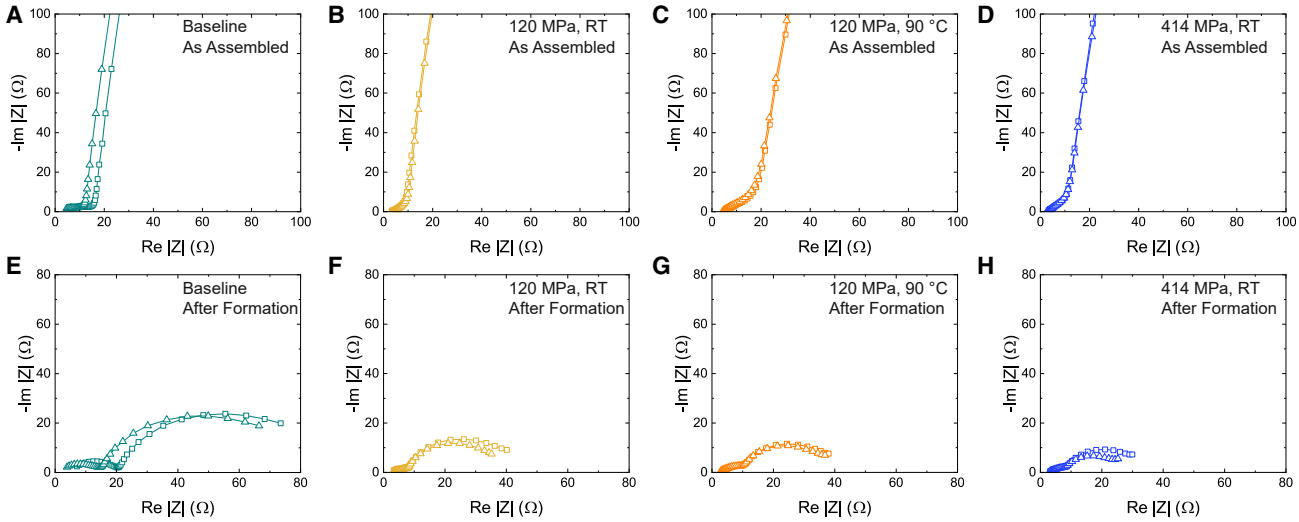

Figure 7. Impedance analysis of coin cells assembled from baseline and ISP-processed electrodes

Shown are impedance spectra of the as-assembled and formation-cycled full cells fabricated with cathode and anode films from the (A and E) baseline material and the ones extracted from the dummy pouch cells that underwent isostatic pressing under (B and F) 120 MPa, RT; (C and G) 120 MPa, 90°C; and (D and H) 414 MPa, RT conditions. See also Figure S13.

showed around 86% retention. It should be noted that the electrochemical performance of these isostatically pressed samples was tested over multiple coin cells, which showed similar performance.

A key benefit of the improved calendaring afforded by the isostatic pressing is potentially improving the power performance of the cells. This was verified by evaluating the rate performance at C/3, 1C, and 3C for the baseline electrode and the cell isostatically pressed at 414 MPa, RT (Figures 10 and S15). At C/3, the baseline electrode and the isostatically pressed electrode show similar performance, as already showcased earlier (Figure 8). However, when increasing the rate to 1C, we see a clear improvement in the capacity attained as well as the retention for the isostatically pressed samples compared to the baseline material. At 1C, the isostatically pressed sample showed 5% higher capacity after 25 cycles and at 3C showed 10% higher capacity after 25 cycles. This is consistent with the impedance results, which showed lower interfacial resistance for the isostatically pressed samples. In general, we think that ISP processed materials behave on par with baseline materials. The small window of improvement observed in the rate capabilities could potentially arise from higher densification or from particle breakdown. These results clearly indicate the benefit of isostatic pressing in improving the rate performance of Li-ion batteries.

Limitations of the present study and implications for battery manufacturing

The present study looks at evaluation of current Li-ion battery materials and the impact of ISP processing on the same. While the results are broadly applicable to solid-state battery systems, there a few important caveats that need to be highlighted. First, we note the limited pressure and temperature settings employed in this study. The pressures selected here represent the nominal as well as the outer bounds of the equipment capabilities with CIP and WIP instruments. Our aim was to investigate these metrics as the baseline to assess the impact of ISP on battery materials. It is imperative that a time-temperature-pressure optimization be carried out for a specific chemistry under scrutiny to maximize densification while mitigating detrimental impacts like particle cracking. Further, we do believe that lowering pressures, as well as modifying holding times, can help with mitigating particle cracking specifically for the system that we investigated. Solid-state batteries will eventually have composite cathodes, metal or metal alloy anodes, as well as solid separators, which might be ceramic or hybrid or amorphous in nature. Mechanical properties of solid ion conductor additives in the cathode are expected to modify the resultant microstructures of the composite cathodes. However, we can safely predict the

Table 1. Comparison of individual resistance components for all four different types of samples

	Before formation cycling			After formation cycling		
Conditions	R1/Ω	R2/Ω	R3/Ω	R1/Ω	R2/Ω	R3/Ω
Baseline	5.1350	8.3560	4.0000	5.4810	6.4590	8.1720
120 MPa RT	3.9040	1.2670	1.7880	2.0510	4.1360	0.99620
120 MPa 90°C	5.3760	2.0000	5.4300	2.7810	3.5720	2.0810
414 MPa RT	3.1870	2.5120	1.3640	2.6080	1.3480	2.3880

Please cite this article in press as: Dixit et al., Isostatic pressing of multilayer pouch cells and its implications for battery manufacturing, Device (2024), https://doi.org/10.1016/j.device.2024.100370

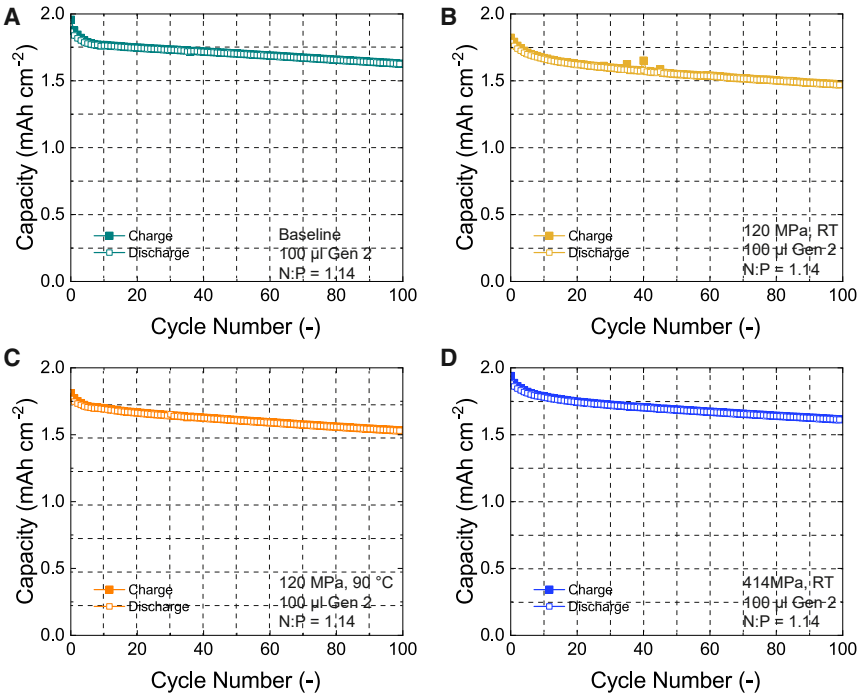

Figure 8. Electrochemical performance of coin cells assembled from baseline and single-layer, ISP processed electrodes

Shown is the cycling performance of cells fabricated with cathode and anode films from the (A) baseline material and the ones extracted from the dummy pouch cells that underwent isostatic pressing under (B) 120 MPa, RT; (C) 120 MPa, 90°C; and (D) 414 MPa, RT conditions. The cycling was carried out with a C/3-C/3 protocol at 30°C. See also Figures S14 and S15.

relative orders of densification using our study as a baseline. Further, initial results with isostatic pressing of Li metal indicates that, below a threshold thickness, creep is negligible, which is consistent with the knowledge in the literature. These results indicate that ISP processing and metal anode thicknesses will need to be carefully tailored to avoid shorting through creep-like phenomena. Finally, we acknowledge that ISP, by definition, is a batch process. However, we believe that this process can neatly dovetail with the current manufacturing line-up in the integration and formation steps. Currently, the formation and aging steps in the Li-ion battery manufacturing process are the greatest bottleneck in terms of time and materials due to extended holds required for adequate wetting as well as a finite number of cycling channels available for formation. We believe that integrating ISP into the process chain at this stage will be ideal for maintaining the production throughput in manufacturing plants. In addition, solid-state batteries, in principle, can be bipolarly stacked, leading to the concept of "cell-to-pack," decreasing the number of cells that need to be processed. Also, formation cycles are likely to be less intensive in SSBs due to the Li metal anode concept. Overall, there are still a lot of questions to be answered with regard to production line integration, but we firmly believe that there are techno-economic benefits to integrate ISP within the processing chain.

The impact of isostatic pressing was studied extensively with dummy multilayer pouch cells. Subsequently, the electrodes from the isostatically pressed pouches were extracted and compared to the baseline electrodes using extensive morphological as well as electrochemical testing. Pressure distributions across the multilayer films are established to be extremely uniform, even for pouch cells containing up to 40 individual layers. This emphasizes the scalability of the ISP process for large form-factor cells. Morphological characterization suggests that some structural damage does occur to the cathode particles after ISP processing; however, it does not adversely impact the performance. Peel tests for adhesion indicate that the ISP-processed samples achieve an order of magnitude higher bonding of the cathode coating to the current collector compared to baseline materials. The isostatically pressed samples retain identical electrochemical performance at nominal C-rate cycling conditions of C/3. At higher rates, slight improvements in the retention and capacity are observed for the isostatically pressed material due to improved calendaring of the electrodes. While we believe that the ISP calendaring technology would be ideal for single-crystal NMC electrodes, our future endeavors will focus on optimizing ISP pressing conditions to avoid particles cracking across all types of cathodes. The findings of this research open new avenues for the development of innovative and scalable battery manufacturing techniques. ISP emerges as a promising technology to address the challenges associated with conventional manufacturing processes, such as porosity control and electrode density optimization, as well as for use in solid-state battery manufacturing.

EXPERIMENTAL PROCEDURES

Resource availability

Lead contact

Requests for further information and additional details should be directed to and will be fulfilled by the lead contact, Marm Dixit (dixitmb@ornl.gov).

Materials availability

Information regarding any data and materials used in this study is available from the lead contact upon reasonable request.

Data and code availability

- No code was used for this study. All data are reported within the supplemental information.
- The process flow and experimental pathway followed for this work are shown schematically in Figure S1A. Dummy cells were manufactured at the Battery Manufacturing Facility at ORNL and subsequently subjected to various ISP protocols. After this, the dummy cells were disassembled, individual layers were extracted, and subsequent testing was carried out on these extracted films.

Please cite this article in press as: Dixit et al., Isostatic pressing of multilayer pouch cells and its implications for battery manufacturing, Device (2024), https://doi.org/10.1016/j.device.2024.100370

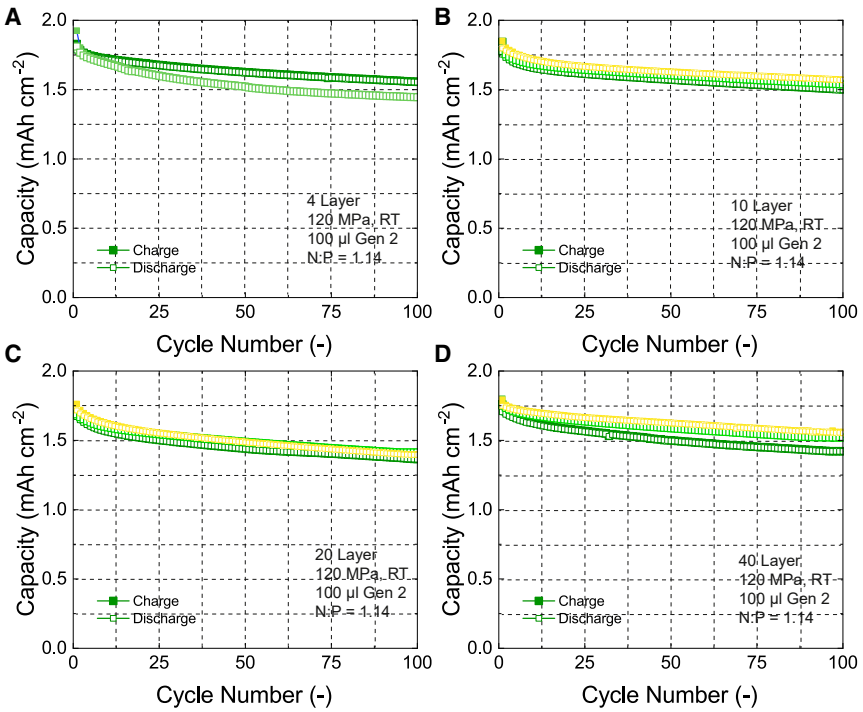

Figure 9. Electrochemical performance of coin cells assembled from multilayer, ISP-processed electrodes

Shown is the cycling performance of cells fabricated with cathode and anode films extracted from the (A) first and second layers of the 4-layer dummy cell; (B) first, fifth, and 10th layers of the 10-layer dummy cell; (C) first, 10th, and 20th layers of the 20-layer dummy cell; and (D) first, 20th, and 40th layers of the 40-layer dummy cell. The multilayer cells were all isostatically processed at 120 MPa, RT. The cycling was carried out with a C/3-C/3 protocol at 30°C. See also Figures S16 and S17.

Fabrication of the dummy pouch cells

The cathode material used was a polycrystalline NMC622 that was sourced from Targray. The graphite used for this study was SLC1520T, sourced from Superior Graphite. The separator material employed was Celgard 2325, which was 25 μm thick. Commercial NMC622 and graphite material were used without any further treatment. Cathode slurries were prepared using N-methylpyrrolidone (NMP). The NMP-processed slurry consisted of 90 wt % NMC cathode active material, 5 wt % carbon black, and 5 wt % polyvinylidene fluoride (PVDF) binder. The anode slurry was prepared by combining 92 wt % graphite, 6 wt % PVDF, and 2 wt % carbon black. To coat the electrodes, a pilot-scale slot-die coater (Frontier) was used. Cathodes were coated onto aluminum foil at loadings ranging from 11.3 to 11.6 mg/cm^2, while anodes were coated onto copper foil at a loading of 7.5 mg/cm^2. All electrodes underwent calendering to achieve a porosity of approximately 35%. Finally, secondary drying was performed either at 115°C (for NMP processed) in a vacuum oven before cell assembly. Single- and multilayer pouch cells were assembled in a dry room with ~0.3% relative humidity. For all cells, Celgard 2325 was used as the separator material. A pressure-sensing film with the range of 7,100–18,500 psi (49–127 MPa) was placed between each layer of the dummy cell. No liquid electrolyte was introduced into the cell before sealing it. Cells with 2 layers (anode and cathode), 4 layers (2× anode and cathode), 10 layers (5× anode and cathode), 20 layers (10× anode and cathode), and 40 layers (20× anode and cathode) were assembled in this fashion.

The typical use of these pressure films is to create an instant, permanent image of pressure variation. These are very commonly used to measure pressing forces in bolted joints, welding fixtures, and jigs. The differences in intensity of the film color depicts the range of pressure observed (Figure S1B). Overall, the aim of the pressure film images extracted from the single- and multilayer stacks was to identify whether there are pressure pinch points observed after ISP treatment. To simplify the visualization with multilayer stacks, the intensity average of the electrode film was evaluated using a custom MATLAB routine.

Isostatic pressing protocol

CIP and WIP of the assembled dummy pouch cells were carried out using a Quintus Laboratory WIP system. The pouch cells were double bagged and vacuum sealed in plastic bags before the ISP treatment. The protocols employed for the different pouch cells are detailed in Table 2. For all cycles, the samples were loaded to the maximum pressure value and held for 5 min, followed by a slow pressure release. For the cell processed at 90°C, the temperature of the chamber was raised to the target value before pressurization. The sealed samples were subsequently opened in the dry room for subsequent characterization.

Fabrication of coin cells and electrochemical testing

Electrodes to make coin cells were extracted from the baseline electrode foils (no ISP treatment) as well as those extracted from the dummy cells that underwent various types of ISP processing. For multilayer cells, representative electrodes from the first, middle, and last layer were punched. The cathode and anode were punched to a diameter of 14 and 16 mm, respectively. Full coin cells were assembled in an argon-filled glove box by pairing the cathodes with the corresponding pressed anode. For all cells, Celgard 2325 was used as the separator material, and 1.2 M $LiPF_6$ in 3:7 wt % ethylene carbonate/ethyl methyl carbonate was used as the electrolyte. To aid in the comparison of data, an equal quantity of 100 μL electrolyte was added to each coin cell. Full coin cells were cycled between 3 V and 4.2 V vs. Li/Li+. Three formation cycles were performed for each cell (C/10 charge, C/10 discharge) before cycle life testing. Cycle life testing was performed by charging and discharging at C/3 for 100 cycles. All tests were conducted in an environmental chamber (Espec) at 30°C using a Maccor battery cycler (Series 4000).

Characterization

The SEM images of the extracted electrodes were taken on a Thermo Fisher Scientific Scios 2 FIB-SEM instrument. XRD patterns of the extracted cathode materials were collected using a Panalytical Empyrean diffractometer employing Cu Kα radiation under 45 kV and 40 mA conditions. The data were collected at RT over the 2θ angle range of 30°–60° with a step size of 0.01°. FIB-SEM images of the processed and baseline cathodes were collected using the Scios2 FIB-SEM instrument. Subsequent data analysis on the collected 3D stack was carried out using Avizo and custom MATLAB routines. The adhesion strength was evaluated using a peel tester (Mecmesin-Friction Peel Tear) equipped with a 100N module. Figure S10 provides a visual depiction of the peel test setup, including a digital photo of the equipment and a magnified image highlighting the different components involved. To measure the adhesion strength, 2.0-cm wide strips of cathodes were cut. 2.4-cm-wide double-sided tape (3M) was placed on the steel plate of the peel tester. The cathode strip was then attached to this double-sided tape, ensuring that the cathode side adhered to the tape while the current collector side faced upward. A 25-pound weight was applied to the affixed cathode for 1.0 min. Subsequently, the metal plate with the attached cathode was securely fastened to the peel tester, and a 2.0-cm-wide single-sided tape was adhered to the current collector of the cathode. The single-sided tape was then pulled using a 100N module.

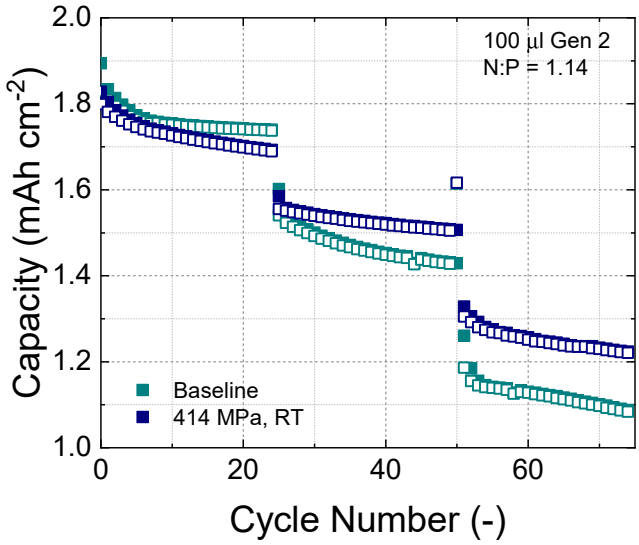

Figure 10. Rate performance studies
Shown is the discharge rate performance of the baseline electrodes and the electrodes extracted from the ISP-processed dummy cell at 414 MPa, RT. The cells are tested with C/3, 1C, and 3C for 25 cycles at each C rate. See also Figure S18.

SUPPLEMENTAL INFORMATION

Supplemental information can be found online at https://doi.org/10.1016/j.device.2024.100370.

ACKNOWLEDGMENTS

This research was conducted at Oak Ridge National Laboratory, managed by UT Battelle, LLC, for the US Department of Energy (DOE) under contract DE-AC05-00OR22725. M.D. was also supported by an Alvin M. Weinberg Fellowship at the Oak Ridge National Laboratory. The work was sponsored by the Laboratory Directed Research and Development (LDRD) Program at Oak Ridge National Laboratory. The US Government retains for itself, and others acting on its behalf, a paid-up, nonexclusive, irrevocable worldwide license in said article to reproduce, prepare derivative works, distribute copies to the public, and perform publicly and display publicly, by or on behalf of the Government. DOE will provide public access to these results of federally sponsored research in accordance with the DOE Public Access Plan (http://energy.gov/downloads/doe-public-access-plan).

AUTHOR CONTRIBUTIONS

M.D., conceptualization, data curation, formal analysis, investigation, methodology, writing – original draft, and writing – review & editing; C.B., R.E., A.B., R.A., M.L., and J.S., formal analysis, investigation, methodology, writing – original draft, and writing – review & editing; T.R., conceptualization, resources, formal analysis, and writing – review & editing; M.B. and I.B., conceptualization, writing – review & editing, funding acquisition, resources, and supervision.

Table 2. Conditions for isostatic pressing for dummy pouch cells

Pouch	Pressure, MPa (KSI)	Temperature (°C)	Time (min)	Medium
2 layer	120 (17.4)	RT	5	oil
2 layer	414 (60)	RT	5	oil
2 layer	120 (17.4)	90 (194°F)	5	oil
4 layer	120 (17.4)	RT	5	oil
10 layer	120 (17.4)	RT	5	oil
20 layer	120 (17.4)	RT	5	oil
40 layer	120 (17.4)	RT	5	oil

DECLARATION OF INTERESTS

The authors declare no competing interests.

Received: January 29, 2024
Revised: April 2, 2024
Accepted: April 9, 2024
Published: May 24, 2024

REFERENCES

1. Deng, J., Bae, C., Denlinger, A., and Miller, T. (2020). Electric Vehicles Batteries: Requirements and Challenges. Joule *4*, 511–515. https://doi.org/10.1016/j.joule.2020.01.013.
2. Li, M., Feng, M., Luo, D., and Chen, Z. (2020). Fast Charging Li-Ion Batteries for a New Era of Electric Vehicles. Cell Rep. Phys. Sci. *1*, 100212. https://doi.org/10.1016/j.xcrp.2020.100212.
3. Zhao, J., Song, C., and Li, G. (2022). Fast-Charging Strategies for Lithium-Ion Batteries: Advances and Perspectives. ChemPlusChem *87*, e202200155. https://doi.org/10.1002/cplu.202200155.
4. Manthiram, A. (2017). An Outlook on Lithium Ion Battery Technology. ACS Cent. Sci. *3*, 1063–1069. https://doi.org/10.1021/acscentsci.7b00288.
5. Wood, D.L., Li, J., and An, S.J. (2019). Formation Challenges of Lithium-Ion Battery Manufacturing. Joule *3*, 2884–2888. https://doi.org/10.1016/j.joule.2019.11.002.
6. Parikh, D., Christensen, T., and Li, J. (2020). Correlating the influence of porosity, tortuosity, and mass loading on the energy density of LiNi0.6Mn0.2Co0.2O2 cathodes under extreme fast charging (XFC) conditions. J. Power Sources *474*, 228601. https://doi.org/10.1016/j.jpowsour.2020.228601.
7. Schmitt, M., Baunach, M., Wengeler, L., Peters, K., Junges, P., Scharfer, P., and Schabel, W. (2013). Slot-die processing of lithium-ion battery electrodes—Coating window characterization. Chem. Eng. Process: Process Intensif. *68*, 32–37. https://doi.org/10.1016/j.cep.2012.10.011.
8. Liu, Y., Zhang, R., Wang, J., and Wang, Y. (2021). Current and future lithium-ion battery manufacturing. iScience *24*, 102332. https://doi.org/10.1016/j.isci.2021.102332.
9. Zaman, W., and Hatzell, K.B. (2022). Processing and manufacturing of next generation lithium-based all solid-state batteries. Curr. Opin. Solid State Mater. Sci. *26*, 101003. https://doi.org/10.1016/j.cossms.2022.101003.
10. Janek, J., and Zeier, W.G. (2023). Challenges in speeding up solid-state battery development. Nat. Energy *8*, 230–240. https://doi.org/10.1038/s41560-023-01208-9.
11. Schnell, J., Günther, T., Knoche, T., Vieider, C., Köhler, L., Just, A., Keller, M., Passerini, S., and Reinhart, G. (2018). All-solid-state lithium-ion and lithium metal batteries – paving the way to large-scale production. J. Power Sources *382*, 160–175. https://doi.org/10.1016/j.jpowsour.2018.02.062.
12. Mauger, A., Julien, C.M., Paolella, A., Armand, M., and Zaghib, K. (2019). Building Better Batteries in the Solid State: A Review. Materials *12*, 3892.
13. Lu, Y., Zhao, C.-Z., Yuan, H., Hu, J.-K., Huang, J.-Q., and Zhang, Q. (2022). Dry electrode technology, the rising star in solid-state battery industrialization. Matter *5*, 876–898. https://doi.org/10.1016/j.matt.2022.01.011.
14. Li, G., Wang, S., Fu, J., Liu, Y., and Chen, Z. (2023). Manufacturing High-Energy-Density Sulfidic Solid-State Batteries. Batteries *9*, 347.

15. Wang, C., Kim, J.T., Wang, C., and Sun, X. (2023). Progress and Prospects of Inorganic Solid-State Electrolyte-Based All-Solid-State Pouch Cells. Adv. Mater. *35*, 2209074. https://doi.org/10.1002/adma.202209074.

16. Dixit, M., Parejiya, A., Essehli, R., Muralidharan, N., Haq, S.U., Amin, R., and Belharouak, I. (2022). SolidPAC is an interactive battery-on-demand energy density estimator for solid-state batteries. Cell Reports Physical Science *3*, 100756.

17. Dixit, M.B., Park, J.-S., Kenesei, P., Almer, J., and Hatzell, K.B. (2021). Status and prospect of in situ and operando characterization of solid-state batteries. Energy Environ. Sci. *14*, 4672–4711.

18. Dixit, M.B., Zaman, W., Bootwala, Y., Zheng, Y., Hatzell, M.C., and Hatzell, K.B. (2019). Scalable manufacturing of hybrid solid electrolytes with interface control. ACS Appl. Mater. Interfaces *11*, 45087–45097.

19. Dixit, M., Beamer, C., Amin, R., Shipley, J., Eklund, R., Muralidharan, N., Lindqvist, L., Fritz, A., Essehli, R., Balasubramanian, M., and Belharouak, I. (2022). The Role of Isostatic Pressing in Large-Scale Production of Solid-State Batteries. ACS Energy Lett. *7*, 3936–3946.

20. Wei, X., Zhang, M., Miao, B., and Liu, R. (2021). Volumetric capacity enhancement in LiFePO4 cathodes by hot isostatic pressing. Scripta Mater. *194*, 113638. https://doi.org/10.1016/j.scriptamat.2020.113638.

21. Lee, Y.-G., Fujiki, S., Jung, C., Suzuki, N., Yashiro, N., Omoda, R., Ko, D.-S., Shiratsuchi, T., Sugimoto, T., Ryu, S., et al. (2020). High-energy long-cycling all-solid-state lithium metal batteries enabled by silver–carbon composite anodes. Nat. Energy *5*, 299–308. https://doi.org/10.1038/s41560-020-0575-z.

22. Fiedler, M., Cangaz, S., Hippauf, F., Dörfler, S., Abendroth, T., Althues, H., and Kaskel, S. (2023). Mechanistic Insights into the Cycling Behavior of Sulfur Dry-Film Cathodes. Advanced Sustainable Systems *7*, 2200439. https://doi.org/10.1002/adsu.202200439.

23. Campéon, B.D.L., Rajendra, H.B., and Yabuuchi, N. (2024). Virtues of Cold Isostatic Pressing for Preparation of All-Solid-State-Batteries with Poly(Ethylene Oxide). ChemSusChem *17*, e202301054. https://doi.org/10.1002/cssc.202301054.

24. Cao, D., Zhao, Y., Sun, X., Natan, A., Wang, Y., Xiang, P., Wang, W., and Zhu, H. (2020). Processing Strategies to Improve Cell-Level Energy Density of Metal Sulfide Electrolyte-Based All-Solid-State Li Metal Batteries and Beyond. ACS Energy Lett. *5*, 3468–3489. https://doi.org/10.1021/acsenergylett.0c01905.

25. David, I.N., Thompson, T., Wolfenstine, J., Allen, J.L., and Sakamoto, J. (2015). Microstructure and Li-Ion Conductivity of Hot-Pressed Cubic $Li_7La_3Zr_2O_{12}$. J. Am. Ceram. Soc. *98*, 1209–1214. https://doi.org/10.1111/jace.13455.

26. Grandjean, M., Perrey, M., Randrema, X., Laurier, J., Chenevier, P., Haon, C., and Liatard, S. (2023). Low pressure cycling of solid state Li-ion pouch cells based on NMC – Sulfide – Nanosilicon chemistry. J. Power Sources *585*, 233646. https://doi.org/10.1016/j.jpowsour.2023.233646.

27. Jiang, B., Wei, Y., Wu, J., Cheng, H., Yuan, L., Li, Z., Xu, H., and Huang, Y. (2021). Recent progress of asymmetric solid-state electrolytes for lithium/sodium-metal batteries. Inside Energy *3*, 100058. https://doi.org/10.1016/j.enchem.2021.100058.

28. Li, C., Zhang, S., Miao, X., Wang, C., Wang, C., Zhang, Z., Wang, R., and Yin, L. (2022). Designing Lithium Argyrodite Solid-State Electrolytes for High-Performance All-Solid-State Lithium Batteries. Batteries & Supercaps *5*, e202100288. https://doi.org/10.1002/batt.202100288.

29. Li, J., Li, Y., Zhang, S., Liu, T., Li, D., and Ci, L. (2023). Long cycle life all-solid-state batteries enabled by solvent-free approach for sulfide solid electrolyte and cathode films. Chem. Eng. J. *455*, 140605. https://doi.org/10.1016/j.cej.2022.140605.

30. Zahiri, B., Patra, A., Kiggins, C., Yong, A.X.B., Ertekin, E., Cook, J.B., and Braun, P.V. (2021). Revealing the role of the cathode–electrolyte interface on solid-state batteries. Nat. Mater. *20*, 1392–1400. https://doi.org/10.1038/s41563-021-01016-0.

31. Shi, F., Pei, A., Vailionis, A., Xie, J., Liu, B., Zhao, J., Gong, Y., and Cui, Y. (2017). Strong texturing of lithium metal in batteries. Proc. Natl. Acad. Sci. USA *114*, 12138–12143. https://doi.org/10.1073/pnas.1708224114.